Efficient intrinsic spin relaxation in graphene due to flexural distortions

S. Fratini (1), D. Gosálbez-Martínez (2) , P. Merodio Cámara (1,3), J. Fernández-Rossier (2,4)
(1) Institut Néel-CNRS and Université Joseph Fourier,
Boite Postale 166, F-38042 Grenoble Cedex 9, France
(2) Departamento de Física Aplicada, Universidad de Alicante, 03690 San Vicente del Raspeig, Spain
(3) SPINTEC, UMR CEA/CNRS/UJF-Grenoble 1/Grenoble-INP, INAC, Grenoble, France
(4) International Iberian Nanotechnology Laboratory (INL),
Av. Mestre José Veiga, 4715-330 Braga, Portugal
(Dated: February 29, 2012)

We propose an intrinsic spin scattering mechanism in graphene originated by the interplay of atomic spin-orbit interaction and the local curvature induced by flexural distortions of the atomic lattice. Starting from a multiorbital tight-binding Hamiltonian with spin-orbit coupling considered non-perturbatively, we derive an effective Hamiltonian for the spin scattering of the Dirac electrons due to flexural distortions. We compute the spin lifetime due to both flexural phonons and ripples and we find values in the 1-10 ns range at room temperature. The proposed mechanism dominates the spin relaxation in high mobility graphene samples and should also apply to other planar aromatic compounds.

PACS numbers:

Introduction. The electron spin lifetime in carbon materials is expected to be very long both because of the very large natural abundance of the spinless nuclear isotope ^{12}C and the small size of spin orbit coupling. In the case of flat graphene, the spin projection perpendicular to the plane is conserved, even in the presence of the intrinsic spin-orbit coupling. Thus, graphene was proposed as an optimal material to store quantum information in the spin of confined electrons [1]. Experiments [2–7] show that the spin lifetimes are much shorter than expected from these considerations, which is conventionally attributed to the combination of two extrinsic factors: the breaking of reflection symmetry due to coupling of graphene to a substrate [8] and/or a gate field, and the breaking of translational invariance due to impurities [9].

Here we propose a radically different scenario: efficient spin relaxation is intrinsic to graphene due to the interplay between its unique mechanical and electronic properties. We show that flexural distortions, unavoidable in two dimensional crystals [10] in the form of either static ripples or phonons, induce spin scattering between the Dirac electrons, to linear order in the flexural field. This coupling differs from the spin-conserving second-order interaction between Dirac electrons and flexural distortions [11] that has been proposed as an intrinsic limit to mobility in suspended high quality samples [12, 13].

The fact that curvature enhances spin-orbit scattering has been discussed in the case of carbon nanotubes [14], graphene [15–17] and graphene ribbons [18]. In the present Letter we derive a microscopic Hamiltonian that describes explicitly the spin-flip scattering of electronic states of graphene due to both dynamic and static flexural distortions. We describe graphene by means of a multi-orbital atomistic description that naturally accounts for the two crucial ingredients of the proposed intrinsic spin-phonon coupling: the intra-atomic spin orbit coupling (SOC) and the modulation of the inter-atomic integrals due to atomic displacements. Importantly, both the SOC and the flexural distortions couple the Dirac electrons to higher energy σ bands, in the spin-flip and spin conserving channels respectively. Their combined action results in an effective spin-flip interaction for the Dirac electrons. The spin-flip scattering rates computed from the theory are shown to provide a very efficient intrinsic spin relaxation mechanism in graphene at room temperature, without the need to invoke scattering with impurities or extrinsic SOC. We find that the spin liftetime of electrons depends crucially on the long wavelength mechanical properties of the sample, determined by its coupling to the environment.

Microscopic model. Our starting point is the tight-binding Hamiltonian $\mathcal{H} = \mathcal{H}_{SC} + \mathcal{H}_{SOC}$ for electrons with spin s moving in a lattice of atoms $\vec{r}$, with atomic orbitals o. We write the hopping part as

$$\mathcal{H}_{SC} = \sum_{\vec{r},\vec{r}',o,o',s} H_{o,o'}(\vec{r}-\vec{r}')\Psi^{\dagger}_{\vec{r},o,s}\Psi_{\vec{r}',o',s}. \qquad (1)$$

considering explicitly the dependence of the (spin conserving) inter-atomic matrix elements on the positions of the atoms. The intra-atomic SOC reads

$$\mathcal{H}_{SOC} = \sum_{\vec{r},o,o',s,s'} \lambda\langle\vec{r}o\sigma|\vec{L}(\vec{r})\cdot\vec{S}|\vec{r}o's'\rangle\Psi^{\dagger}_{\vec{r},o,s}\Psi_{\vec{r},o',s'} \qquad (2)$$

where $\vec{S}$ is the spin operator, $\vec{L}(\vec{r})$ is the orbital angular momentum operator acting upon the atomic orbitals of site $\vec{r}$ and λ is the spin-orbit coupling parameter.

Deviations from the ideal graphene lattice affect its electronic properties via modifications of the transfer integrals in Eq. (1). Their dependence on the inter-atomic distance, for example, gives rise to an electron-phonon interaction analogous to that of conducting polymers

[19] and leads to the appearence of effective gauge fields [16, 20]. In the present model, we consider instead the coupling with flexural distortions arising from the *angular* dependence of the interatomic Hamiltonian. We describe corrugations away from perfectly flat graphene in the form $\vec{r} \simeq \vec{r}_0 + h(\vec{r})\hat{z}$, where $\vec{r}_0$ is a vector of the honeycomb lattice and $h(\vec{r})$ is the displacement of atom $\vec{r}$ perpendicular to the graphene sheet. We expand the interatomic Hamiltonian matrix to lowest order in the flexural field $h(\vec{r})$ and rewrite the Hamiltonian as $\mathcal{H} = \mathcal{H}_0 + \mathcal{V}$, where $\mathcal{H}_0$ now describes ideally flat graphene including the weak intra-atomic SOC perturbation, and

$$\mathcal{V} = \sum_{r,r',o,o',s} [h(\vec{r}) - h(\vec{r}')] \frac{\partial}{\partial z} H_{o,o'}(\vec{r}_0 - \vec{r}_0') \Psi^\dagger_{\vec{r},o,s} \Psi_{\vec{r}',o',s}. \tag{3}$$

is the spin-conserving coupling between electrons and corrugations.

Electron-flexural phonon scattering. It is now convenient to recast Eq. (3) in terms of the eigenstates of the Hamiltonian $\mathcal{H}_0$ for flat graphene. In this context, atoms are specified by their unit cell vector, $\vec{R}$, and their position $\vec{r}_\alpha$ inside the cell (sublattice index $\alpha = A, B$). The creation operators for Bloch states are related to atomic orbitals through:

$$c^\dagger_{\nu\vec{k}} = \frac{1}{\sqrt{N}} \sum_{\vec{R},\alpha,o,s} e^{i\vec{k}\cdot\vec{R}} \mathcal{C}_{\nu,\vec{k}}(\alpha, o, s) \Psi^\dagger_{\vec{R}+\vec{r}_\alpha,o,s} \tag{4}$$

where $\vec{k}$ is the wave-vector, the coefficients $\mathcal{C}_{\nu,\vec{k}}(\alpha, o, s)$ are obtained from the diagonalization of the Bloch matrix and ν is an index that labels the resulting bands (with mixed spin and angular momentum). Similarly, we expand the flexural field on each sublattice in its Fourier components, $h_\alpha(\vec{R}) = \frac{1}{\sqrt{N}} \sum_{\vec{q}} e^{-i\vec{q}\cdot\vec{R}} h_\alpha(\vec{q})$. After a lengthy but straightforward calculation, we can express Eq. (3) as a term causing scattering between crystal states with different momentum and band index:

$$\mathcal{V} = \sum_{\vec{k},\vec{k}',\nu,\nu'} \mathcal{V}_{\nu,\nu'}(\vec{k},\vec{k}') c^\dagger_{\nu,\vec{k}} c_{\nu',\vec{k}'} \tag{5}$$

$$\mathcal{V}_{\nu,\nu'}(\vec{k},\vec{k}') \equiv \frac{1}{\sqrt{N}} \sum_{\vec{R},\alpha,\alpha',o,o',\sigma} \frac{\partial}{\partial z} H_{o,o'}(\vec{r}_\alpha - \vec{r}_{\alpha'} - \vec{R}) \times \\ \times F^{\vec{R}}_{\alpha\alpha'}(\vec{k},\vec{k}') \mathcal{C}^*_{\nu,\vec{k}}(\alpha, o, \sigma) \mathcal{C}_{\nu',\vec{k}'}(\alpha', o', \sigma) \tag{6}$$

The coupling is *linear* in the flexural phonon field, through the form factor $F^{\vec{R}}_{\alpha\alpha'}(\vec{k},\vec{k}') = h_\alpha(\vec{k}-\vec{k}')e^{i\vec{k}'\cdot\vec{R}} - h_{\alpha'}(\vec{k}-\vec{k}')e^{i\vec{k}\cdot\vec{R}}$. This should be contrasted with the electron-flexural phonon coupling usually considered within the π subspace [11–13, 20], that is quadratic in the field because of the quadratic dependence of interactomic distances on h. Note that $H_{oo'}$ is short ranged within our tight-binding description, which limits $\vec{R}$ to the 4 vectors connecting neighboring cells (inter-cell coupling), as illustrated in Fig. 1a, plus the null vector (intra-cell coupling).

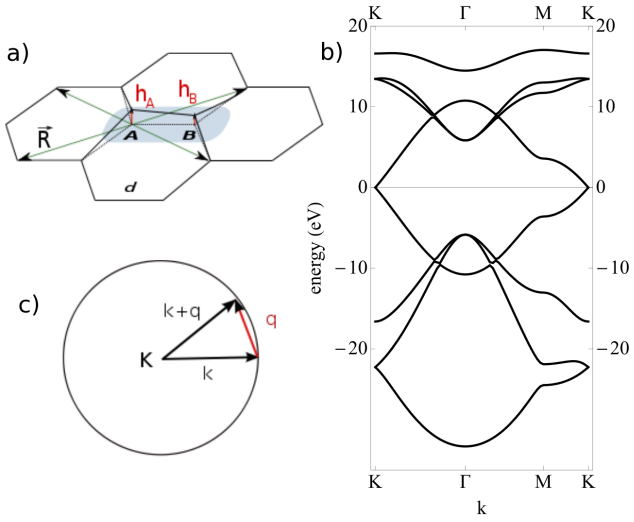

FIG. 1: (a) Sketch of a local corrugation of the graphene layer. The shaded area is the unit cell. Green arrows indicate the inter-atomic contributions to the electron-flexural phonon coupling of Eq. (6). (b) The band structure resulting from our Slater-Koster parametrization (c) Kinematics of the scattering process around the Dirac point K in the low phonon frequency limit.

Slater-Koster parametrization. Equations (5,6) provide a general recipe to compute the coupling of electrons of a generic tight-binding Hamiltonian to a flexural field. We now show that because we have included the SOC in the reference Hamiltonian $\mathcal{H}_0$, the perturbation Eq. (5) is able to induce a direct coupling between states with opposite spin. Following previous work [14, 15, 17, 18, 22] we consider a subset of 4 valence orbitals of the Carbon atom, namely $o = s, p_x, p_y, p_z$, and adopt a Slater-Koster (SK) [21] parametrization for the tight-binding Hamiltonian Eq. (1) [23]. In this framework, the interatomic matrix elements $H_{o,o'}$ connecting the atom α at $\vec{r}_\alpha$ with atom α' at $\vec{r}_{\alpha'} + R$ can be expressed in terms of 4 parameters, V_{ss}, V_{sp}, $V_{\sigma\pi}$, $V_{\pi\pi}$, describing inter-orbital overlaps in the s, p basis [18, 21], and the three director cosines l, m, n of the interatomic bond vectors $\vec{\rho} = \vec{r}_\alpha - \vec{r}_{\alpha'} - \vec{R}$, defined by $\vec{\rho} \equiv \rho\,(l\hat{x} + m\hat{y} + n\hat{z})$. Setting $U_x \equiv V_{pp\pi} + x^2 V_{\sigma\pi}$ and $V_{\sigma\pi} \equiv (V_{pp\sigma} - V_{pp\pi})$ we can write the SK matrix in compact form as

$$H(\vec{\rho}) = \begin{pmatrix} V_{ss\sigma} & lV_{sp\sigma} & mV_{sp\sigma} & nV_{sp\sigma} \\ -lV_{sp\sigma} & U_l & lmV_{\sigma\pi} & lnV_{\sigma\pi} \\ -mV_{sp\sigma} & lmV_{\sigma\pi} & U_m & mnV_{\sigma\pi} \\ -nV_{sp\sigma} & lnV_{\sigma\pi} & mnV_{\sigma\pi} & U_n \end{pmatrix} \tag{7}$$

The unperturbed crystal states for flat graphene are described by $H(\vec{\rho})$ with $n = 0$ (all bonds within the x, y plane). The resulting band structure is shown in Fig.

1b. From Eq. (6), the electron-flexural distortion coupling is determined by $\partial_z H(\vec{\rho}) = (1/d)\partial_n H(\vec{\rho})$, where d is the equilibrium C-C distance. Direct inspection of Eq. (7) shows that $H(\vec{\rho})(n=0)$ does not couple the p_z and s, p_x, p_y sectors, while $\partial_n H(\vec{\rho})$ does. As a result, the π and σ bands of flat graphene are not mixed in the absence of SOC, unless they scatter with flexural distortions. In the presence of SOC, however, the π states with spin s mix with the σ states with opposite spin already within the reference $\mathcal{H}_0$ for flat graphene. Close to the Dirac points, where the π and σ bands are separated in energy by a gap $E_{\sigma\pi}$, the spin $\pi-\sigma$ mixing is proportional to $\lambda/E_{\sigma\pi}$. Since this correction is small, the low energy Dirac bands of $\mathcal{H}_0$ can still be labeled according to their dominant spin character, that we denote as $\Uparrow$ and $\Downarrow$.

The above derivation shows that there are two perturbations that couple π and σ states, the spin-conserving coupling to the flexural field, and the spin-flip SOC. Their combination is able to yield a spin-flip channel within the low energy π bands, that is linear in both the flexural deformation and in the atomic spin-orbit coupling λ, in contrast with the λ^2 perturbation that applies to flat graphene [15].

Spin-flip rates. We now apply the microscopic theory developed above to compute the spin relaxation rate for electrons close to the Dirac points. Anticipating that the dominant contributions to spin-flip scattering arise from the long-wavelength, low energy flexural modes, we consider the lower flexural branch for which $\omega_q \propto q^2$ (see below), discarding the higher energy modes that involve out of phase vibrations of the two sublattices. The flexural field is factored out from Eq. (5) by setting $h_A(\vec{q}) = h_{\vec{q}}$ and $h_B(\vec{q}) = e^{i\vec{q}\cdot(\vec{r}_B - \vec{r}_A)} h_{\vec{q}}$, which yields:

$$\mathcal{V} = \sum_{\vec{k},\vec{q},\nu,\nu'} M_{\nu,\nu'}(\vec{k},\vec{q}) \frac{h_{\vec{q}}}{d} c^\dagger_{\nu,\vec{k}+\vec{q}} c_{\nu',\vec{k}} \tag{8}$$

with $\mathcal{V}_{\nu,\nu'}(\vec{k}+\vec{q},\vec{k}) = \frac{h_{\vec{q}}}{d} M_{\nu,\nu'}(\vec{k},\vec{q})$. The standard form for the phonon spin-flip interaction in second quantization is readily obtained by substituting $h_{\vec{q}} = \sqrt{\frac{\hbar}{2M_C\omega_{\vec{q}}}}(a^\dagger_{-\vec{q}} + a_{\vec{q}})$ into Eq. (8), with M_C the Carbon mass.

The spin relaxation rate can now be calculated from Eq. (8) via the Fermi golden rule. Because the dispersion of the flexural modes is much weaker than the electronic dispersion, we can safely neglect the phonon frequency in the energy conservation. The relaxation rate for an electron with momentum $\vec{k}$ in the band $\Uparrow$ is then obtained by summing over both phonon absorption and emission processes and over all possible final states in the $\Downarrow$ band, which yields:

$$\Gamma_{\vec{k}} = \frac{2\pi}{\hbar} \int \frac{d^2q}{(2\pi)^2} |M_{\Uparrow,\Downarrow}(\vec{k},\vec{q})|^2 \langle h^2_{\vec{q}}\rangle \delta(E_{\vec{k}+\vec{q}} - E_{\vec{k}}). \tag{9}$$

This, together with the explicit expressions for the spin-flip matrix elements in Eq. (6), constitutes the main result of this work. From Eq. (9) it is clear that once that the specific form of the electron-flexural phonon coupling, $M_{\Uparrow,\Downarrow}(\vec{k},\vec{q})$, is known, the behavior of the spin relaxation rate is fully determined by by the statistical fluctuations of the flexural field, $\langle h^2_{\vec{q}}\rangle$. Interestingly, the above expression describes on an equal footing both low-frequency flexural modes (that arise in free-standing or weakly bound graphene or graphite) as well as static ripples (relevant to graphene deposited on a substrate). The proposed spin relaxation mechanism therefore applies without distinction to both physical situations.

For actual calculations we approximate the π band energies as $E_{\vec{k}} = \pm\hbar v_F |\vec{k}|$, which is valid except for a negligible interval around the Dirac point, where the SOC opens a gap of the order of few μeV. Energy conservation implies $\sqrt{k^2+q^2+2kq\cos\theta} = \sqrt{k^2}$. This fixes the relative angle between $\vec{k}$ and $\vec{q}$ to $\cos\theta = -\frac{q}{2k}$ (see Fig.1c), which allows to perform the angular integration in Eq. (9), yielding:

$$\Gamma_{\vec{k}} = \frac{1}{\pi\hbar} \int_0^{2k} dq \frac{|M_{\Uparrow,\Downarrow}(k,q)|^2 \langle h^2_q\rangle}{\hbar v_F \sqrt{1-(q/2k)^2}}. \tag{10}$$

In principle, the spatial derivative in the electron-phonon coupling elements of Eq. (6) should translate into a linear scaling of the matrix elements $M_{\Uparrow,\Downarrow}$ with exchanged momentum q. This result, however, only holds at the Dirac points, i.e. for $k=0$. From our numerics, we find instead that in the relevant case of small but finite k the matrix elements evaluated on the energy-conserving surface satisfy the non-trivial result:

$$|M_{\Uparrow,\Downarrow}(k,q)|^2 = \lambda^2 (kd)^2 \left(\frac{q}{2k}\right)^4, \tag{11}$$

independent on the SK parameters.

Fluctuations of the flexural field. We now evaluate the flexural fluctuations $\langle h^2_q\rangle$ in different cases of physical interest. We start with the expression for free-standing graphene at thermal equilibrium:

$$\langle h^2_q\rangle = \frac{\hbar}{2M_C\omega_q}[1+2n_B(\omega_q)] \simeq \frac{k_B T}{M_C\omega_q^2}, \tag{12}$$

where $n_B(\omega_q)$ is the thermal population of mode q and the second equality holds when $k_B T \gg \hbar\omega_q$. For purely harmonic flexural modes, for which $\omega_q \simeq Dq^2$, the fluctuation $\langle h^2_{\vec{q}}\rangle$ diverges as q^{-4} for small q. This divergence is renormalized due to the interaction with other phonons (i.e. by anharmonic effects) [24], and can be further cut off by the presence of strain [13] or pinning to a substrate [25]. The resulting dispersion can be written in general as $\omega_q = D\sqrt{q^4 + q^{4-\eta} q_c^\eta}$ so that, in the long wavelength limit,

$$\langle h^2_q\rangle \propto \frac{1}{q^{4-\eta} q_c^\eta} \tag{13}$$

where η and q_c depend on the physical mechanism of renormalization. Specifically, substrate pinning opens a gap in the phonon spectrum [25], corresponding to $\eta = 4$; strain makes the dispersion linear at long wavelengths [13] ($\eta = 2$); anharmonic effects yield $\eta = 0.82$ [24].

Based on the asymptotic long-wavelength behavior Eq. (13) we obtain the following general expression for the spin relaxation rate in terms of the scaling parameter η, momentum k, and cutoff q_c, valid for $k \lesssim q_c$:

$$\Gamma_k = \frac{\lambda^2}{E_k} \frac{\langle h_{1/d}^2 \rangle}{d^2} \frac{F_\eta}{8\pi\hbar} \left(\frac{2k}{q_c} \right)^\eta \qquad (14)$$

where $F_\eta = (\sqrt{\pi}/2)\Gamma[(1+\eta)/2]/\Gamma[1+\eta/2]$ is a constant of order 1 and $\langle h_{1/d}^2 \rangle / d^2 = k_B T (d^2/M_C D)$ is a dimensionless measure of the C-C bond angle fluctuations [from Eq. (12), evaluated at $q = 1/d \gg q_c$]. The spin relaxation rate increases linearly with temperature, following the thermal population of flexural phonons. A weaker temperature dependence arises when anharmonic effects dominate, because the anharmonic cutoff is itself temperature dependent, $q_c \propto \sqrt{T}$ [10, 24].

Interestingly, substituting the Fermi wavevector $k_F = \sqrt{\pi n}$ into the above expression results in a density depencence $\Gamma_{k_F} \propto n^{(\eta-1)/2}$ (which is valid for $E_F \gtrsim k_B T$). Therefore, the spin relaxation rate can either be an increasing or decreasing function of doping depending on the value of η, which is ultimately determined by the mechanical environment of graphene. At high density ($k_F \gg q_c$), instead, the cut-off becomes negligible and the integral in Eq. (10) converges to the result for ideal graphene [Eq. (14) with $\eta = 0$] regardless of the value of η. In view of these results, and because the proposed flexural spin relaxation mechanism is essentially independent from the spin-conserving scattering that determines the electrical mobility, some care should be taken when identifying the spin relaxation mechanism (Elliot-Yafet, or Dyakonov-Perel) from the relative scaling of the spin and momentum relaxation rates with carrier density, as is customarily done [6, 7, 16, 31].

Results and discussion. The spin lifetime $\tau_s = 1/\Gamma_{k_F}$ obtained from Eq. (10) for electrons at the Fermi level is plotted as a function of electron density in Fig. 2. We take $D = 4.6 \cdot 10^{-7} m^2 s^{-1}$ [13], $\lambda = 8$ meV [26], $T = 300K$ and $v_F = 1.16 \cdot 10^6 m/s$ from our SK band structure. Different curves correspond to different values of the scaling exponent η, i.e. to physically different mechanical environments for graphene. Two representative values of the cutoff momentum, $q_c = 0.01$ Å^{-1} and $q_c = 0.1$ Å^{-1} are considered, covering the large spread of q_c values available in the literature. In both panels, the result for ideal graphene in the harmonic approximation is shown for reference (black) as it provides an absolute lower bound to the actual lifetime.

In the density range relevant to current graphene-based devices, the predicted spin lifetime is typically in the range of 1-10 ns at room temperature. Because the spin relaxation is dominated by the low energy fluctuations of the membrane, the shortest spin lifetimes are obtained in suspended unstrained graphene (red curve), i.e. when external mechanical influences are minimized and the mobility is possibly largest. This should also apply to the case of graphene on boron nitride [27], where the substrate is atomically flat and effectively decoupled from the graphene layer. All in all, considering the electronic mobilities currently reachable in suspended graphene $\mu = 2 \cdot 10^5 cm^2/Vs$ ($6 \cdot 10^4 cm^2/Vs$ in the case of BN substrates [27]) our theoretical predictions for the spin lifetime set an intrinsic limit to the spin relaxation length in excess of $L_s \approx 10\mu m$ at room temperature.

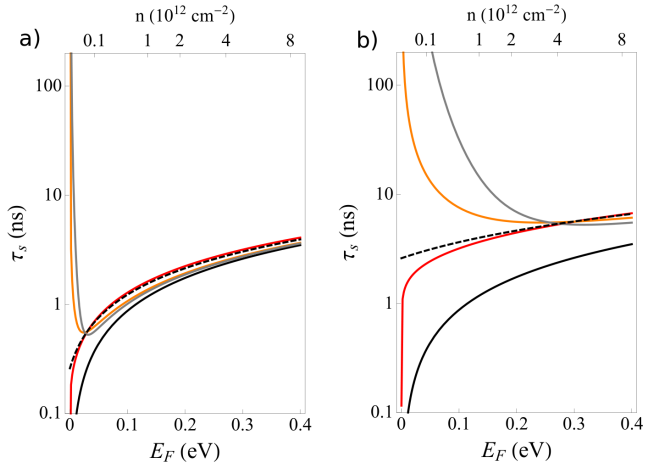

FIG. 2: Room temperature spin lifetime calculated from the theory for electrons at the Fermi energy, for 2 different values of cutoff momentum: (a) $q_c = 0.01$ Å^{-1} and (b) $q_c = 0.1$ Å^{-1} (right) and different long-wavelength scaling laws: ideal graphene (black, $\eta = 0$); including anharmonic effects (red, $\eta = 0.82$); including strain (orange, $\eta = 2$) and substrate pinning (gray, $\eta = 4$). The black dashed line is for $\eta = 1$, which is representative for substrate roughness.

Longer spin lifetimes could be achieved by suppressing the fluctuations of the graphene membrane, by an applied strain (orange) [13] or substrate pinning (gray) (similarly, the proposed mechanism would be clearly ineffective in epitaxially grown graphene due to the strong interlayer binding). We note however that while quenching dynamical fluctuations, the coupling to a substrate may introduce static corrugations, which are also detrimental to the spin lifetime. This could be at the origin of the spin lifetimes measured in graphene on SiO_2 in Ref. [6]. Recent measurements of ripples of graphene on SiO_2 are indeed compatible with $\eta \lesssim 1$ for $q \gtrsim q^* = 0.02$ Å^{-1} [28], which is ascribed to the presence of substrate roughness. At densities such that $k_F > q^*$, the spin relaxation from such ripples is again described by Eq. (14), with now a prefactor $\langle h_{1/d}^2 \rangle / d^2$ determined by the substrate morphology rather than by Eq. (12), that could

in principle be extracted from the experiment.

Concluding remarks. In summary, we have shown that corrugations, that are ubiquitous in graphene in the form of dynamical flexural phonons or static ripples, enable a direct spin-flip mechanism to linear order in both the flexural field and in the spin-orbit coupling. This mechanism provides an efficient source of spin relaxation, setting an intrinsic limit for the spin lifetime in high mobility samples. Such limit is however non-universal, as its precise value depends on graphene's mechanical environment, that determines the long-wavelength behavior of the flexural field. At room temperature, intrinsic spin lifetimes in the nanosecond range are expected in a very wide range of situations. We note that an analogous mechanism could be at the origin of the spin relaxation recently reported in small organic molecules [32], with an enhancement of the spin-orbit coupling caused by the low-frequency molecular bending modes.

Finally, whereas the existence of a rather small upper limit for spin-lifetimes in graphene might present an obstacle for certain applications like spin transistors, the intrinsic spin-lattice coupling could open the way for hybrid devices, where a confined vibrational phonon could be coupled resonantly coupled to the spin-flip transitions of Zeeman split of confined Dirac electrons. Microwave pumping of such system could result in a maser behavior of the phonon mode [33].

Acknowledgements This work has been financially supported by MEC-Spain (MAT07-67845, FIS2010-21883-C02-01, and CONSOLIDER CSD2007-00010) and Generalitat Valenciana (ACOMP/2010/070).

[1] B. Trauzettel, D. V. Bulaev, D. Loss, G. Burkard Nature Physics **3**, 192-196 (2007).
[2] N. Tombros, J. Csaba, M. Popinciuc, J. Mihaita H. T. Jonkman, and B. J. van Wees, Nature **448**, 571 (2007)
[3] N. Tombros, S. Tanabe, A. Veligura, C. Jozsa, M. Popinciuc, H. T. Jonkman, and B. J. van Wees Phys. Rev. Lett. **101**, 046601 (2008)
[4] K. Pi, Wei Han, K. M. McCreary, A. G. Swartz, Yan Li, and R. K. Kawakami Phys. Rev. Lett. **104**, 187201 (2010)
[5] T.- Y. Yang, J. Balakrishnan, F. Volmer, A. Avsar, M. Jaiswal, J. Samm, S. R. Ali, A. Pachoud, M. Zeng, M. Popinciuc, G. Guntherodt, B. Beschoten, and B. Ozyilmaz Phys. Rev. Lett. **107**, 047206 (2011)
[6] Wei Han and R. K. Kawakami Phys. Rev. Lett. **107**, 047207 (2011)
[7] Wei Han, K.M. McCreary, K. Pi, W.H. Wang, Yan Li, H. Wen, J.R. Chen and R.K. Kawakami, J. Magn. Magn. Mater. **324**, 369 (2012)
[8] C. Ertler, S., Konschuh, M. Gmitra, M., J. Fabian, Phys. Rev. B **80**, 041405(R) (2009).
[9] A. H. Castro Neto, F. Guinea, Phys. Rev. Lett. **103**, 026804 (2009).
[10] A. Fasolino, J. H. Los, M. I. Katsnelson Nature Materials **6**, 858 - 861 (2007)
[11] E. Mariani and F. von Oppen Phys. Rev. Lett. **100**, 076801 (2008)
[12] S. V. Morozov, K. S. Novoselov, M. I. Katsnelson, F. Schedin, D. C. Elias, J. A. Jaszczak, and A. K. Geim Phys. Rev. Lett. **100**, 016602 (2008);
[13] Eduardo V. Castro, H. Ochoa, M. I. Katsnelson, R. V. Gorbachev, D. C. Elias, K. S. Novoselov, A. K. Geim, and F. Guinea Phys. Rev. Lett. **105**, 266601 (2010)
[14] T. Ando, J. Phys. Soc. Jpn. **69**, 1757 (2000).
[15] D. Huertas-Hernando, F. Guinea, and A. Brataas, Phys. Rev. B **74**, 155426 (2006)
[16] D. Huertas-Hernando, F. Guinea, A. Brataas, Phys. Rev. Lett. **103**, 146801 (2009).
[17] Jae-Seung Jeong, Jeongkyu Shin, and Hyun-Woo Lee Phys. Rev. B **84**, 195457 (2011)
[18] D. Gosálbez-Martńez, J. J. Palacios, and J. Fernández-Rossier Phys. Rev. B **83**, 115436 (2011)
[19] W. P. Su, J. R. Schrieffer, and A. J. Heeger Phys. Rev. Lett. **42**, 1698 (1979)
[20] A. H. Castro Neto, F. Guinea, N. M. R. Peres, K. S. Novoselov and A. K. Geim, Rev. Mod. Phys. 81, 109 (2009)
[21] J. C. Slater and G. F. Koster Phys. Rev. **94**, 1498 (1954)
[22] H. Min, J. E. Hill, N. Sinitsyn, B. Sahu, L. Kleinman, and A. H. MacDonald, Phys. Rev. B **74**, 165310 (2006)
[23] In the calculations we have left out d orbitals, for simplicity. It has been shown that they give the dominant contribution to the SOC gap at the Dirac points[29, 30], but they do not renormalize the change of the gap with the flexural distortion[29], which is related to the spin-phonon coupling proposed here. In any event, our results provide a lower limit for the instrinsic spin relaxation mechanism, given the fact that including the d orbitals will enhance the effect.
[24] K. V. Zakharchenko, R. Roldán, A. Fasolino, and M. I. Katsnelson Phys. Rev. B **82**, 125435 (2010)
[25] J. Sabio et al., Phys. Rev. B 77, 195409 (2008)
[26] F. Kuemmeth, S. Ilani, D. C. Ralph, and P. L. McEuen, Nature **452**, 448 (2008)
[27] C. R. Dean, et al., Nat. Nano. 5, 722 (2010)
[28] M. Ishigami, et. al, Nano Letters 7, 1643 (2007)
[29] M. Gmitra, S. Konschuh, C. Ertler, C. Ambrosch-Draxl, and J. Fabian Phys. Rev. B **80**, 235431 (2009)
[30] Sergej Konschuh, Martin Gmitra, and Jaroslav Fabian Phys. Rev. B **82**, 245412 (2010)
[31] I. Žutić, J. Fabian and S. Das Sarma, Rev. Mod. Phys. 76, 323 (2004)
[32] L. Schulz et al., Phys. Rev. B 84, 085209 (2011)
[33] I. Bargatin and M. L. Roukes Phys. Rev. Lett. **91**, 138302 (2003)